



1 **Morphology of GPS and DPS-TEC Over an Equatorial Station:**
2 **Validation of IRI and NeQuick 2 Models.**

3 4 Olumide O. Odeyemi¹, Jacob Adeniyi², Olushola Oladipo³, Olayinka Olawepo³, Isaac Adimula³, Elijah Oyeyemi¹

5 ¹ Department of Physics, University of Lagos, Nigeria olumidephysics@yahoo.com, oodeyemi@unilag.edu.ng

6 ² Department of Physical Sciences, Landmark University, Omu-Aran, Nigeria adeniyi.jacob@lmu.ng.edu

7 ³ Physics Department, University of Ilorin, Ilorin

8 Correspondence to: Olumide O. Odeyemi (olumidephysics@yahoo.com)

9
10 **0.0 Abstract**

11 We investigated total electron content (TEC) at Ilorin (8.50°N 4.65E, dip lat. 2.95) during
12 a low solar activity 2010. The investigation involved the use of GPS derived TEC, TEC
13 estimated from digisonde portable sounder data (DPS-TEC), the International Reference
14 Ionosphere model (IRI-TEC) and NeQuick 2 model (NeQ-TEC). The five most quietest days of
15 the months obtained from the international quiet days (IQD) from the website
16 http://www.ga.gov.au/oracle/geomag/iqd_form.jsp were used for the investigation. During the
17 sunrise period, we found that the rate of increases in DPS-TEC, IRI-TEC and NeQ-TEC were
18 higher with respect to GPS-TEC. One reason for this can be alluded to an overestimation of
19 plasmaspheric electron content (PEC) contribution in modeled TEC and DPS-TEC. A correction
20 factor around the sunrise where a significant percentage difference of overestimations between
21 the modeled TEC and GPS-TEC was obtained will correct the differences. Our finding revealed
22 that during the daytime when PEC contribution is known to be absent or insignificant, GPS-TEC
23 and DPS-TEC in April, September and December predicts TEC very well. The lowest
24 discrepancies were observed in May, June and July (June solstice) between the observed and all
25 the model values in all hours. There is an overestimation in DPS-TEC that could be due to
26 extrapolation error while integrating from the peak electron density of F2 (NmF2) to around ~
27 1000 km in the Ne profile. The underestimation observed in NeQ-TEC must have come from the
28 inadequate representation of contribution from PEC on the topside of NeQ model profile
29 whereas the exaggeration of PEC contribution in IRI-TEC amount to overestimations of GPS-
30 TEC. The excess bite-out observed in DPS-TEC and NeQ-TEC show the indication of
31 overprediction of fountain effect in these models. Therefore, the daytime bite-out observed in
32 these two models require a modifier that could moderate the perceived fountain effect
33 morphology in the models accordingly. Seasonally, we found that all the TECs maximize and
34 minimize during the March equinox and June solstice, respectively. Therefore, GPS-, DPS-, IRI-



35 and NeQ-TEC reveal the semi-annual variations in TEC as reported in all regions. The daytime
36 DPS-TEC performs better than the daytime IRI-TEC and NeQ-TEC in all the months, however,
37 the dusk period requires attention due to highest percentage difference recorded especially for
38 DPS-TEC and the models in March, and November and December for DPS-TEC.

39

40 1.0 Introduction

41 Total electron content (TEC) is the total number of free electrons in a columnar of one
42 square meter along the radio path from the global positioning system (GPS) satellite to the
43 receiving station on the Earth. TEC exhibits diurnal, seasonal, solar cycle and geographical
44 variations. Therefore, the physical and dynamical morphology of the TEC over a given location
45 is of great importance in trans-ionospheric communications during undisturbed and disturbed
46 geomagnetic conditions (Jesus et al., 2016; Tariku, 2015; and Akala et al., 2012). GPS-TEC is
47 quantified from the GPS orbiting satellites to the GPS receiver station on the Earth, with an
48 approximate distance of 20200 km (Liu et al., 1996b; Rama Rao et al., 2006a; Rama Rao et al.,
49 2006b; Liu et al., 2006). Thus, a typical GPS-TEC measurement includes the complete
50 plasmaspheric electron content (PEC).

51

52 The International Reference Ionosphere (IRI) is a standard model that is based on
53 worldwide data from various measurements (Bilitza, 2001; Bilitza, 1999; Bilitza, 1986; Bilitza
54 and Rawer, 1998; and Rawer et al., 1978). The Committee on Space Research (COSPAR) and
55 the Union Radio-Scientifique Internationale (URSI) meet yearly to improve the IRI model. The
56 IRI model provides reliable ionospheric densities, composition, temperatures, and composition
57 (Bilitza, 2001). The Comite Consultatif International des Radiocommunications (CCIR) Model
58 was developed by Rawer and Bilitza (1990) while the Union Radio Scientific International
59 (URSI) developed URSI option of IRI model (Fox and McNamara, 1988; Rush et al., 1989). The
60 latest version of IRI model can be found at all time on the web
61 (<http://nssdc.gsfc.nasa.gov/space/model/ions/iri.html>) with improvements on earlier versions of
62 the model from the working group scientists on the model. The International Telecommunication
63 Union, Radio-communication Sector (ITU-R) has introduced and adopted NeQuick for TEC
64 modeling. In the NeQuick 2, the position, time and solar flux or sunspot number over a given
65 location are embedded in the NeQuick model code. The output of the NeQuick 2 program is the



66 electron density along any ray-path while the corresponding TEC measurement is by numerical
67 integration in space and time. The availability ionospheric parameters as contribution for global
68 ionospheric models are not sufficient over the Africa sector compared to the consistent input of
69 the parameters from the Asia and America sectors. Therefore, the investigations of the
70 ionospheric parameters over Africa are continuously required to improve the global ionospheric
71 model. For example, Bagiya et al. (2009) studied TEC around equatorial-low latitude region at
72 Rajkot (22.29° N, 70.74° E, dip 14.03° N) during low solar activity and showed that TEC
73 revealed seasonal variation with maximum and minimum at March equinox and June solstice,
74 respectively. Young et al. (1970) examined a night enhancement in TEC at equatorial station of
75 Hawaii and reported that the nighttime enhancement in TEC showed seasonal and solar cycle
76 dependences. Olwendo et al. (2012) investigated TEC in Kenyan and found a semi-annual
77 variation with minimum and maximum TEC June solstice and March equinox, respectively.
78 They further reported that the TEC had a noontime dip and day-to-day variability. Using
79 Faraday rotational technique, Olatunji (1967) studied TEC variation over equatorial station at
80 Ibadan and found no daytime bite-out and seasonal anomaly over the equatorial region. Adewale
81 et al. (2012) investigated TEC at Uganda during low and high solar activities. They found that
82 TEC was higher during high solar activity compared with the low solar activity. Karia and
83 Pathak. (2011) investigated the TEC at Surat and showed that TEC maximizes and minimizes
84 during the equinox and June solstice, respectively. Rastogi et al. (1975) investigated the diurnal
85 variation of TEC using Faraday rotation over the magnetic equator. They found that the TEC at
86 the topside was higher than the TEC at the bottomside during the nighttime, however during the
87 daytime, equal distribution of TEC was found on the topside and the bottomside of electron
88 density (Ne) profile.

89

90 The DPS-TEC is the combination of TEC from the bottomside and topside electron
91 density (Ne). The topside DPS-TEC is an extrapolated TEC from the peak electron density of
92 the F2 region ($NmF2$) to around~ 1000 km (DPS-TEC) thus, the major PEC contribution from
93 the greater altitudes is excluded from DPS-TEC measurement (Belehaki et al., 2004; Breed and
94 Goodwin, 1997; and Reinisch and Huang, 2001). The combined investigation on GPS and DPS
95 is scanty over Africa (Ciraolo and Spalla, 1997) due to lack of colocated GPS and DPS data in
96 most of the equatorial stations. Therefore, the ionospheric modeling and the improvement on the



97 existing models are important to understanding of the ionospheric structure of a given location in
98 the absence of instrumentations.

99 Regarding the DPS-TEC measurement, Barbas et al. (2010) investigated GPS-TEC and
100 DPS-TEC at Tucuman (26.69° S, 65.23° W) during different seasons and magnetic activities.
101 They concluded that the DPS-TEC variation represented the GPS-TEC in all hour with minimal
102 discrepancy. Reinisch et al.(2004) investigated GPS-TEC from satellite beacon signals and
103 DPS-TEC from the DPS at mid-latitude and equatorial region. They found that GPS-TEC and
104 DPS-TEC variations were similar. However, the daytime GPS-TEC profile values were higher
105 than DPS-TEC profile values. Belehaki et al. (2004) extracted the plasmaspheric electron
106 content (PEC) from the GPS-TEC at Athens (38° N, 23.5° E) over a year and found a maximum
107 and minimum contribution of PEC in the morning and evening, respectively. Zhang et al. (2004)
108 investigated the simultaneous variation of DPS-TEC and GPS-TEC over Hainan and reported
109 that the daytime DPS-TEC and GPS-TEC variations are close, however during nighttime to pre-
110 sunrise, a significant discrepancy between DPS-TEC and GPS-TEC was observed. Mosert and
111 Altadill (2007), Jodogne et al. (2004) and Mckinnell et al. (1996) concluded that estimated
112 PEC from the GPS-TEC and DPS-TEC is possible in colocated GPS and DPS station.

113
114 Rios et al. (2007) investigated the DPS-TEC and IRI-TEC and found a smaller DPS-TEC
115 compared to IRI TEC in all hour. McNamara (1985) observed discrepancies between DPS-TEC
116 and IRI-TEC, he found that during the daytime, the IRI underestimated the observed DPS-TEC.
117 Obrou et al. (2008) compared the DPS-TEC and IRI-TEC at Korhogo during high and low solar
118 activity. They found that DPS-TEC and IRI-TEC values were close during high solar activity
119 (HSA) and low solar activity (LSA). Nevertheless, the performance between the observed and
120 model TEC was better in HSA compared to LSA. Adewale et al. (2012), Okoh et al. (2014), Jee
121 and Scherliess (2005), Sulungu et al. (2017), and Migoya Orué et al. (2008) validated the IRI-
122 TEC with GPS-TEC in different regions and found high discrepancies between the IRI and
123 observed TEC. Furthermore, Arunpold et al. (2014) and Olwendo et al. (2012; 2013) also
124 concluded that the signature of the geomagnetic storm was absent in the morphology of IRI.
125 Thus IRI-TEC could not predict the effect of the geomagnetic storm on observed TEC.

126



127 Regarding the studies on NeQuick model, Cherniak and Zakharenkova (2016) validated
128 NeQuick model and found that the topside ionosphere above ~ 500km in the NeQuick model
129 consistently revealed underestimation due to inaccurate representation of topside Ne profile.
130 Bidaine and Warnant (2011) validated NeQuick model with slant total electron content (STEC).
131 Rabiu et al. (2014) validated NeQuick model using the seasonal variation of TEC over equatorial
132 station of Africa. They found that the upper boundary of the NeQuick models up to 20,000 km
133 needs to be adjusted to accommodate the PEC-TEC in NeQuick model. Migoya-Orue et al.
134 (2017) introduced B2bot in NeQuick and reported the improvement in the topside performance
135 of the NeQuick model in the computation of TEC. Andreeva and Lokota (2013) found that the
136 NeQuick reproduced the maximum values of electron density observed in the experiments.
137 However, the electron density profiles reproduction from NeQuick show significant
138 discrepancies in some periods. Leong et al. (2013) investigated TEC and NeQuick 2 models.
139 They found that the observed TEC and NeQuick 2 TEC are close in values during post-noon and
140 post-midnight. However, the post-sunset revealed some discrepancies. Yu et al. (2012)
141 investigated the monthly average of NeQuick model over three stations in China (Changchun,
142 Beijing, and Chongqing) during the quietest period. They found that NeQuick accurately
143 predicted GPS-TEC. However, the NeQuick underestimated the observed TEC and NmF2 in
144 few cases.

145

146 The current contributions of Africa on the improvement of ionospheric models (IRI and
147 NeQuick) are not adequate compared with the continuous support received from Asia and South
148 America. The scanty of ionospheric instrumentations at the equatorial region of Africa has a
149 considerable effect on the shortcoming. Therefore, the continuous validation of IRI and NeQuick
150 models with the observed parameter is necessary for improved ionospheric model. Furthermore,
151 the investigation on DPS-TEC has not been reported extensively for comparison purpose.
152 Therefore, this paper set to investigate the combined relationship between the variations of GPS-
153 TEC and DPS-TEC, and validations of IRI-TEC, and NeQ-TEC models with the observed
154 parameters. Our finding will reveal the suitability of DPS-TEC, IRI-TEC and NeQ-TEC in place
155 of GPS-TEC. The result will also reveal the appropriate model for the equatorial station in
156 Africa. Thus, the changed TEC obtained from the combined relationship between GPS-TEC,



157 DPS-TEC, IRI-TEC and NeQ-TEC could be used to improve the discrepancy in the model
158 values.

159

160 2.0 Methods of Analysis of GPS and DPS Data

161 The five most quiet days of GPS and DPS-TEC data for each month were presented and
162 analyzed during the year 2010 with the local time (LT).

163

164 2.1 GPS-TEC

165 The Slant TEC records from GPS has errors due to satellite differential delay (satellite
166 bias (b_s)) and receiver differential delay (receiver bias (b_r)) and receiver inter-channel bias (b_{SR}).
167 This uncorrected slant GPS-TEC measured at every one-minute interval from the GPS receiver
168 derived from all the visible satellites at the Ilorin station are converted to vertical GPS-TEC
169 using the relation below in equation (1).

170
$$(GPS - TEC)_V = (GPS - TEC)_S - [b_s + b_r + b_{SR}] / S(E) \quad 1$$

171 Where $(GPS - TEC)_S$ is the uncorrected slant GPS-TEC measured by the receiver, $S(E)$ is the
172 obliquity factor with zenith angle (z) at the Ionospheric Pierce Point (IPP), E is the elevation
173 angle of the satellites in degrees and $(GPS - TEC)_V$ is the vertical GPS-TEC at the IPP. The
174 $S(E)$ is given as

175

176
$$S(E) = \frac{1}{\cos \frac{\pi z}{180}} = \left[1 - \left(\frac{R_E \times \cos \frac{\pi z}{180}}{R_E + h_s} \right)^2 \right]^{-1/2} \quad 2$$

177 Where R_E is the mean radius of the Earth measured in kilometer (km), and h_s is the height of the
178 ionosphere from the surface of the Earth, which is approximately equal to 400 km according to
179 Langley et al. (2002) and Mannucci et al. (1993). The ten most quiet slant GPS-TEC data for
180 each month in the year 2010 were analyzed using Krishna software. This software reads raw data
181 and corrects all source of errors mentioned above from Global Navigation Satellite System
182 service (IGS) code file. A minimum elevation angle of 20 degrees is used to avoid multipath
183 errors. The estimated vertical GPS-TEC data is subjected to a two sigma (2σ) iteration. This
184 sigma is a measure of GPS point positioning accuracy. The average one-minute VTEC data were
185 converted to hourly averages.

186



187 **2.2 DPS-TEC**

188 Regarding the total electron content (TEC) from the digisonde portable sounder (DPS),
189 the Standard Archive Output (SAO) files obtained from the recorded of ionogram from the
190 installed DPS at the University Ilorin were edited to remove magnetically disturbed days. Huang
191 and Reinisch (2001) technique was used to compute the DPS-TEC. The complete vertical DPS-
192 TEC computation is obtained by applying the integration over the vertical electron density
193 (Ne(h)) profile as shown in the equation below.

194
$$\text{TEC} = \int_0^{\text{hmF2}} \text{Ne}_B(\text{dh}) + \int_{\text{hmF2}}^{\infty} \text{Ne}_T(\text{dh}) \quad 3$$

195 Where Ne_B and Ne_T are the bottomside and topside Ne profiles, respectively. The Ne_B is
196 computed from the recorded ionograms by using the inversion technique developed by Huang
197 and Reinisch (1996). It is known that the information above the peak of the F2 layer is absent
198 from the record of the ionogram. Thus the Ne_T is computed by approximating the exponential
199 functions with suitable scale height (Bent et al., 1972) with less estimated error of 5%. The
200 ionograms are manually scaled and inverted into electron density profile using the NHPC
201 software and later processed with the SAO explorer software based on the technique described
202 above to obtain the TEC (Reinisch et al., 2005). An average of TEC for each hour is computed
203 over the selected days. The universal time (UT) is the time convention for these analyses (GPS
204 and DPS data). Local time (LT) was used in this study. Thus, 0100 UT (Universal time) is the
205 same as 0200 LT (Local Time) in Nigeria. In this study, the seasonal variation was arranged into
206 four seasons, as, March equinox or MEQU (March, and April), June solstice or JSOL (June, and
207 July), SEQU (September, and October) and December solstice or DSOL (November, December).
208 Due to technical reasons, there were data gaps in all days during January and February in the
209 DPS measurements, therefore, we decided to neglect data in January and February in GPS-, IRI-,
210 and NeQuick measurements for comparison purposes thus, two simultaneous representative
211 months were used to infer each season. The average of the monthly median of the five quietest
212 days for the representative months is found to give each parameter a particular season discussed
213 above.

214

215 **2.3 Validation of IRI - 2016 and NeQuick Models**

216 The observed TEC and NmF2 were compared with the IRI-2016 model. The website
217 http://www.ccmc.gsfc.nasa.gov/modelweb/models/iri_vitmo.php provides the modeled TEC



218 values. The upper boundary height 2000 km was used, and the B0 table option was selected for
219 the bottomside shape parameter. The equations 3a, 3b and 3c represent the difference between
220 GPS-TEC and DPS-TEC, GPS-TEC and IRI-TEC and GPS-TEC and NeQ-TEC while equations
221 4a, 4b, and 4c below show the percentage change between GPS-TEC and DPS-TEC, GPS-TEC
222 and IRI-TEC, and GPS-TEC and NeQ-TEC.

223

224 $\Delta_{\text{GPS/DPS}} = \text{DPS}_{\text{TEC}} - \text{GPS}_{\text{TEC}}$ 3a

225 $\Delta_{\text{GPS/IRI}} = \text{IRI}_{\text{TEC}} - \text{GPS}_{\text{TEC}}$ 3b

226 $\Delta_{\text{GPS/NeQ}} = \text{NeQ}_{\text{TEC}} - \text{GPS}_{\text{TEC}}$ 3c

227 $\%(\Delta_{\text{GPS/DPS}}) = \frac{\text{DPS}_{\text{TEC}} - \text{GPS}_{\text{TEC}}}{\text{DPS}_{\text{TEC}}} \times 100$ 4a

228 $\%(\Delta_{\text{GPS/IRI}}) = \frac{\text{IRI}_{\text{TEC}} - \text{GPS}_{\text{TEC}}}{\text{IRI}_{\text{TEC}}} \times 100$ 4b

229 $\%(\Delta_{\text{GPS/NeQ}}) = \frac{\text{NeQ}_{\text{TEC}} - \text{GPS}_{\text{TEC}}}{\text{NeQ}_{\text{TEC}}} \times 100$ 4c

230 $\Delta_{\text{GPS/DPS}}$, represents the change between GPSTEC and DPS-TEC

231 $\Delta_{\text{GPS/IRI}}$, represents the change between GPS-TEC and IRI-TEC

232 $\Delta_{\text{GPS/NeQ}}$ represents the change between GPS-TEC and NeQ-TEC

233 $\%(\Delta_{\text{GPS/DPS}})$, represents the percentage deviation between GPS-TEC, and DPS-TEC
234 respectively.

235 $\%(\Delta_{\text{GPS/IRI}})$, represents the percentage deviation between GPS-TEC, and IRI-TEC respectively.

236 $\%(\Delta_{\text{GPS/NeQ}})$, represents the percentage deviation between GPS-TEC, and NeQ-TEC
237 respectively.

238

239 The Abdus Salam International Centre for Theoretical Physics (ICTP) - Trieste, Italy
240 with the collaboration of the Institute for Geophysics, Astrophysics and Meteorology (IGAM) of
241 the University of Graz, Austria developed the web front-end of NeQuick. This quick-run
242 ionospheric electron density model developed at the Aeronomy and Radiopropagation
243 Laboratory modeled TEC along any ground-to-satellite straight line ray-path. Therefore, the
244 observed TEC use for the validation of the NeQuick 2 was obtained in the address below
245 <https://t-ict4d.ictp.it/nequick2/nequick-2-web-model>.

246



247 **3.0 Result**

248 **3.1 Monthly Median Variations**

249 Figure 1 shows the plots of diurnal variations of the monthly median of GPS-, DPS-, IRI-
250 , and NeQ- TEC during quiet period. The GPS-TEC is plotted in black line with the star symbol;
251 the DPS-TEC is in green with the diamond symbol, IRI-TEC is in red line with zero symbols,
252 and finally, the NeQ-TEC is in blue line with multiplication symbol. All TEC plots are regulated
253 by the same local time (LT) on the horizontal axis. We found that the variations of GPS-, DPS-,
254 IRI, and NeQ-TEC increase gradually from the sunrise period and reach the daytime maximum,
255 then later decay till it gets to a minimum around 0500 or 0600 LT. These results show that the
256 models capture the well known solar zenith angle dependence of TEC. Regarding the GPS-TEC,
257 the pre-sunrise minimum is ranged between ~0.43 TECU (June) to ~2.35 TECU (April) and the
258 sunrise minimum of ~ 1.76 TECU, ~ 2.58 TECU, and ~ 2.58 TECU are observed in March,
259 November, and December respectively. The daytime maximum ranged between ~ 20 TECU
260 (June) - ~ 35.4 TECU (November) and occurred around 1500 - 1700 LT. The dusk time decay
261 in GPS-TEC is faster in June and slower in November around 2400 LT. Regarding DPS-TEC,
262 the pre-sunrise minimum of DPS-TEC ranged between ~ 0.66 TECU (August) - ~ 4.59 TECU
263 (May) around 0500 LT, while the daytime maximum is found around 1000 - 1600 LT and
264 ranged between ~ 24.2 TECU (July) - ~ 38.0 TECU (March). A moderate daytime bite-out in
265 DPS-TEC was observed in March, May, August, September, October, November and December.
266 The duration of the bite-out was longer in October (1000 -1600 LT). The decay of DPS-TEC is
267 faster in June and lower in April. Regarding the IRI-TEC, the pre-sunrise minimum in IRI-TEC
268 ranged between ~ 2.3 TECU (March) - ~ 4.1 TECU (October and November) and found around
269 0500 LT. The daytime maximum is seen around 1500 LT and 1600 LT and ranged between ~
270 21.9 TECU (July) - ~31.7 TECU (November). A moderate bite-out is present in all months
271 between 1100 - 1600LT. As regard NeQ-TEC, the pre-sunrise minimum ranged between ~ 1.31
272 TECU (July) - ~ 2.88 TECU (December) and found around 0500 LT. The daytime maximum
273 around 1000 LT and 1600 LT, ranged between ~ 17.75 TECU (July) - ~ 25.45 TECU
274 (November). A moderate noon time bite-out is seen in May, June, July, and August within a
275 short time range. The decay in NeQ-TEC is faster in July and slower in November.
276 Our investigation reveals that GPS, DPS, IRI and NeQ-TEC decay is faster and slower in June
277 and December seasons, respectively. The maximum daytime is found in the DPS-TEC, whereas



278 the minimum daytime is observed in NeQ-TEC. The DPS-TEC show a higher pre-sunrise
279 minimum of ~ 4.59 TECU (May) while the GPS-TEC revealed a smaller pre-sunrise minimum
280 of ~ 0.43 TECU (June).

281

282 **3.2 Percentage deviation of DPS-TEC**

283 Figures 2a, and 2b show hourly variations of the changed TEC, and mass plot of hourly
284 variations of % changed TEC between GPS-TEC and DPS-TEC from March to December
285 during quiet period. Between 0100 - 0500 LT (Figure 2a), DPS-TEC constantly lower than the
286 GPS-TEC in March, April, August, September, November, and December except in June and
287 July and the changes range between ~ -4.67 TECU (November) - ~ -0.53 TECU (August). In
288 Figure 2b, DPS-TEC uniformly overestimated GPS-TEC around 0700 - 1500 LT in all month
289 except in June (0700 LT), November (1500 LT), August and December (1400 - 1500 LT) where
290 DPS-TEC underestimated GPS-TEC. The percentage of overestimation ranges between $\sim 2\%$
291 (November) - $\sim 49\%$ (March). We also observed that the DPS-TEC underestimated GPS-TEC
292 between 1700 - 2400 LT in all months and ranged between $\sim -0.15\%$ (October) - $\sim -306\%$
293 (November). A few cases of overestimation are noticed in March, May and September around
294 local time (1700 LT). We also notice a consistent overestimation of DPS-TEC around 0100 LT
295 and 0400 LT in June and July while underestimation occurred in March, April, August,
296 September, October, November and December within the same period.

297

298 **3.2 Percentage deviation of IRI-TEC**

299 Figures 3a, and 3b, give hourly variations of the changed TEC, and mass plots of hourly
300 variations of % changed TEC between GPS-TEC and IRI-TEC from March to December. The
301 change between IRI-TEC and GPS-TEC occurred between 0100 - 1200 LT in all months except
302 in March and April and the changed TEC ranged between ~ 0.01 TECU (November) to ~ 15
303 TECU (October). The IRI-TEC continually overestimated GPS-TEC around 0100 - 1200 LT in
304 all months however, underestimation occurred in March (0100 - 0500 LT), April (1200 LT),
305 September and November (0300 - 0400 LT). The overestimation percentage ranges between \sim
306 0.1% (December) - $\sim 86\%$ (June) between 0100 - 1200 LT. We also observed that in May and
307 June, IRI-TEC overestimated GPS-TEC during May and June in all hours between $\sim 2\%$ (1900
308 LT) and $\sim 86\%$ (0500 LT), respectively. Between 1300 - 2400 LT, we observed some irregular



309 patterns of underestimation and overestimation of DPS-TEC over GPS-TEC in most of the
310 months.

311

312 **3.4 Percentage deviation of NeQ-TEC**

313 Figures 4a, and 4b, reveal the hourly variations of the changed TEC, and mass plots of
314 hourly variation of % changed TEC between GPS-TEC and NeQ-TEC from March to December
315 during quiet period. The increase change between NeQ-TEC and GPS-TEC are found 0100 -
316 0900 LT except in November and December. We also found that, NeQ-TEC constantly
317 overestimated GPS-TEC around 0100 - 0900 LT in all month except in March, April, August,
318 September and November around 0400 LT and also around 0500 LT in March, April and
319 November. The overestimation percentage is ranged between ~ 0.02% (April) - ~ 81% (July).
320 We also observed that the NeQ-TEC underestimated GPS-TEC between 1200 - 1900 LT in all
321 months and ranged between ~ - 0.3% (October) - ~ - 75% (November). In July, we noticed a
322 consistent overestimation of NeQ-TEC in all hours except around 1300 LT (~ - 1.5%) and 1400
323 LT (~ - 0.6%) . Between 2000 - 2400 LT, NeQ-TEC overestimated GPS-TEC in March, April,
324 June, September, October and December whereas in May, July, August and November, NeQ-
325 TEC underestimated GPS-TEC.

326

327 **3.5 Comparisons of the deviations from GPS-TEC**

328 From Figure 2b, 3b, and 4b, we constantly found high percentage of underestimations of
329 DPS-TEC, IRI-TEC and NeQ-TEC with respect to GPS-TEC between 0400 - 0600 LT in March
330 and December. Around 0100 - 0500 LT, highest DPS-TEC percentage of underestimation are ~
331 190%, ~ 210% - ~ 280% in March, November, and December respectively, highest IRI-TEC
332 percentage of underestimation of IRI-TEC is ~ 200% in March, and highest NeQ-TEC
333 overestimations is ~ 68% and ~75% in June and July, respectively and highest underestimation
334 is ~ 60% in March. Between 0700 LT - 1800 LT, DPS-TEC overestimation and underestimation
335 ranges between ~ 10% - ~ 10% in all months, IRI-TEC overestimation and underestimation
336 ranges between ~ 70 - ~ 50% in all months, and NeQ-TEC overestimation and underestimation
337 of ranges between ~ 80% - ~ 80% in all months. During 1900 - 2400 LT, DPS-TEC highest
338 underestimation is ~ 310% in March, IRI-TEC overestimation and underestimation are found
339 between the range of ~ 50% - ~ 50% in all months, and NeQ-TEC overestimation and



340 underestimation ranges between $\sim 70\%$ - $\sim 70\%$ in all months. Figure 5 reveals the seasonal
341 variations of GPS-TEC, DPS-TEC, IRI-TEC, and NeQ-TEC during quiet period. We observed
342 that both DPS-TEC and models reproduce the semi-annual variation with maximum and
343 minimum TEC at March equinox and June solstice, respectively. The daytime maximum is
344 ranged between ~ 24.8 TECU (NeQ) - ~ 34 TECU (DPS), ~ 19.2 TECU (NeQ) - ~ 22.6 TECU
345 (DPS), ~ 24.9 TECU (NeQ) - ~ 33.5 TECU (DPS) and ~ 24.55 TECU (NeQ) - ~ 31 TECU
346 (DPS), in March equinox, June solstice, September equinox, and December solstice,
347 respectively.

348

349 **4.0 Discussion of Result**

350 An investigation into the variations of GPS-TEC, DPS-TEC, IRI-TEC, and NeQ-TEC at
351 an equatorial station (8.5^0N 4.65^0E) in Africa during low solar activity in the year 2010 has been
352 carried out. The TEC increases gradually from the sunrise period, then slowly reached the
353 daytime maximum, and later decay till the pre-sunrise minimum. This result indicates that the
354 TEC is a solar zenith angle dependence revealing maximum and minimum in TEC during the
355 noontime and pre-sunrise or sunrise minimum, respectively (Wu et al. 2008; Aravindan and Iyer
356 1990; and Kumar and Singh 2009). Interestingly, the faster increase in the DPS-TEC than GPS-
357 TEC during pre-sunrise is not consistent with the findings of Ezquer et al. (1992) at Tucumán
358 (26.9°S ; 65.4°W), Belehaki et al. (2004) at Athens in the middle latitude, McNamara (1985) at
359 low latitude and Obrou et al. (2008) at Korhogo (9.33°N , 5.43°W , Dip = 0.67°S) and found
360 smaller DPS-TEC compared with GPS-TEC. The evidence of PEC on GPS-TEC was recently
361 reported by Belehaki et al. (2004). They extracted the plasmaspheric electron content (PEC)
362 from the GPS-TEC and found a significant PEC in the morning and evening. Also, Jodogne et al.
363 (2004), Mosert and Altadill (2007), and Mckinnell et al. (1996) obtained a rough estimation of
364 PEC from the GPS and DPS-TEC. They concluded that the combined GPS-TEC and DPS-TEC
365 could give the PEC of a given location. Therefore, a larger DPS-TEC during the sunrise could be
366 attributed to inaccurate representation of PEC in the topside DPS-TEC profile during
367 extrapolation from the peak of NmF2 to around ~ 1000 km of Ne profile. Thus, a typical GPS-
368 TEC naturally includes the PEC measurement (Belehaki et al. 2003; Balan and Iyer, 1983;
369 Carlson, 1996; and Breed and Goodwin, 1997).

370



371 Furthermore, our observation in GPS-TEC shows no conspicuous noontime bite-out. The
372 bite-out is attributed to the occurrence of the most active fountain effect during the noontime at
373 the magnetic equator due to the lifting of ionospheric plasma. Thus, the bite-out result from the
374 interaction of eastward electric field and earth horizontal magnetic field. The interactions
375 resulted to the lifting of plasma at the magnetic equator and diffused along geomagnetic field
376 lines into the high latitudes, so leaving the reduced TEC at the magnetic equator
377 (Bandyopadhyay, 1970; Olwendo et al., 2012; Skinner et al., 1966; Bolaji et al., 2012).
378 However, the absence of daytime bite-out (Olatunji, 1967) in GPS-TEC found in our result
379 shows that the productions of the bottomside and topside electron content are enhanced quickly
380 to replenish the loss of the ionization that occurs during the noontime through the fountain effect.
381 The higher DPS-TEC compared with IRI-TEC around sunrise is not consistent with Rios et al.
382 (2007) who investigated comparison of DPS-TEC and IRI-TEC and found that DPS-TEC is
383 smaller than IRI TEC in all hour. They concluded that the prediction of IRI-TEC included the
384 high topside Ne profile. Thus, our observation suggests that the IRI-TEC has included low
385 topside Ne profile in the model or excessive exaggeration of PEC in the topside Ne profile in the
386 DPS-TEC. Our investigation shows that the daytime GPS-TEC and DPS-TEC in April, August
387 and December appear to be approximately equal. This finding suggests that the topside Ne
388 profile in DPS-TEC are moderately captured in the topside Ne profile in GPS-TEC. This finding,
389 thus indicates the absence of PEC profile in DPS-TEC approximately reproduced the daytime
390 GPS-TEC and IRI-TEC (April, August and December). The insignificance of daytime PEC in
391 the observation is inferred from the report of Rastogi et al. (1975) who measured TEC from
392 Faraday rotations from ground receiver to ~ 20200 km. They found that the PEC contribution on
393 the topside and the bottomside Ne profile is insignificant during the daytime. Moreover,
394 Belehaki et al. (2004) investigation has recently reported the negligible PEC contributions during
395 the daytime.
396

397 Our higher daytime DPS-TEC compared with daytime IRI-TEC is consistent with
398 McNamara (1985) who reported higher DPSTEC compared with IRI-TEC during the daytime.
399 However, in the report of Obrou et al. (2008) at the equatorial station, the IRI-TEC was higher
400 than the DPS-TEC at the low solar activity. We found a reduced daytime IRI and NeQ-TEC
401 compared with GPS-TEC that indicates the excessive PEC removal from the model values that



402 its PEC contribution had been initially exaggerated during the sunrise. Our finding is supported
403 by Migoya-Orue et al. (2017), Zakharenkova (2016), Rabiu et al., (2014), Nava and Radicella
404 (2009), and Zh et al. (2014). They concluded that the topside ionosphere in the NeQuick model
405 consistently revealed underestimation of observed TEC. The daytime IRI-TEC (April, July,
406 August, and September) and NeQ-TEC (June) is approximately reproduced in the GPS-TEC;
407 this implies that the model factors in IRI and NeQ perform best in the absence of significant
408 PEC contribution.

409

410 The hourly variations of percentage difference between GPS-TEC and DPS-TEC, GPS-
411 TEC and IRI-TEC and GPS-TEC and NeQ-TEC in all months revealed that the pre-sunrise
412 values in DPS-TEC, IRI-TEC and NeQ-TEC require an attention due to high percentage
413 difference recorded in all variations especially in March for DPS-TEC and the models, and
414 November and December for DPS-TEC. The daytime DPS-TEC value is closer to the GPS-TEC
415 value compared to the daytime IRI-TEC and NeQ-TEC values. The nighttime NeQ-TEC and
416 IRI-TEC perform better with GPS-TEC compared with DPS-TEC in all months, however more
417 improvement is also required to minimize the effect of the discrepancies observed during the
418 night. More work needs to be done during the pre-sunrise in all models especially in March for
419 all models, and November and December for DPS-TEC.

420

421 Seasonally, we discovered that TEC is maximum and minimum during the equinoxes and
422 the solstices, respectively. Our report is consistent with Mala et al. (2009), Wu et al. (2008),
423 Kumar and Singh (2009), and Balan and Rao, (1984) who investigated TEC in various regions.
424 They concluded that the seasonal variation in TEC is attributed to the seasonal differences in
425 thermospheric composition. Moreover, the sub-solar point is around the equator during the
426 equinox. Consequently, the sun shines directly over the equatorial region, and in addition to the
427 high ratio of O/N₂ around the region, this translates to stronger ionization, thus, semi-annual
428 pattern is formed. Our finding is supported by Ross Skinner et al. (1966), Bolaji et al. (2012),
429 and Scherliess and Fejer (1999) who obtained semi-annual variation in TEC. Scherliess and Fejer
430 (1999) suggested that daytime $E \times B$ drift velocities result to semi-annual variation because the
431 drift velocities are more and less significant in the equinoctial months and June solstice,
432 respectively.



433

434 **5.0 Conclusion**

435 An investigation into the quietest GPS-TEC, DPS-TEC, IRI-TEC, and NeQ-TEC over an
436 equatorial station of Africa during just ascending phase cycle of low solar activity in the year
437 2010 was carried out. Our findings indicate that the variations in GPS, DPS, IRI, and NeQ-TEC
438 are solar zenith angle dependence having maximum and minimum TEC during the noontime and
439 pre-sunrise or sunrise minimum. We also found that the absence of daytime bite-out in the GPS-
440 TEC is exaggerated in the DPS-TEC, IRI-TEC, and NeQ-TEC morphologies. Furthermore, our
441 result reveals a faster sunrise increase in DPS-TEC, IRI-TEC, and NeQ-TEC than GPS-TEC that
442 is attributed to the misinterpretation of the topside Ne profile of the DPS-TEC, IRI-TEC, and
443 NeQ-TEC in order to incorporate the plasmaspheric electron content (PEC) into the models. The
444 daytime DPS-TEC is also higher than the daytime GPS-TEC, IRI-TEC, and NeQ-TEC, except in
445 April, September and December where daytime DPS-TEC and GPS-TEC values are close. The
446 daytime GPS-TEC is also approximately equal the daytime IRI-TEC in April, July, August and
447 September whereas in the daytime NeQ-TEC only June approximately close to the daytime GPS-
448 TEC. The close values in daytime TEC obtained in DPS-TEC and IRI-TEC in some months may
449 be unconnected to the improved model values in the absence or a little PEC contributions during
450 the daytime. Another finding is the faster decay in DPS-TEC during the dusk time compared to
451 GPS-TEC, IRI-TEC, and NeQ-TEC. However, the decline is approximately similar in value
452 found in June, July and August (June solstice). The hourly variations of percentage difference
453 between GPS-TEC and DPS-TEC, GPS-TEC and IRI-TEC and GPS-TEC and NeQ-TEC in all
454 months revealed that the pre-sunrise values in DPS-TEC, IRI-TEC and NeQ-TEC require an
455 attention. The daytime DPS-TEC value is closer to the GPS-TEC value compared to the daytime
456 IRI-TEC and NeQ-TEC values. The nighttime NeQ-TEC and IRI-TEC perform better with
457 GPS-TEC compared with DPS-TEC in all months. This study was carried out during the
458 quietest period of the year 2010; it will be of advantage to investigate the similar work during the
459 most disturbed days and compared with our results. Moreover, additional stations in the
460 equatorial region will be needed to validate the latitudinal effect of the model with the observed
461 parameters. This will reshape the model parameters for improved ionospheric modeling over
462 Africa.

463



464 **6.0 Acknowledgments**

465 We would like to appreciate Massachusetts University and Boston College, respectively
466 for the donations of DPS and GPS facilities to the University of Ilorin, Nigeria. Also, the kind
467 supports of the University of Ilorin in running the DPS and GPS stations and in providing the
468 data for use are gratefully acknowledged and appreciated.

469

470 **7.0 References**

471

472 Adewale, A.O., Oyeyemi, E.O., and Olwendo, J. (2012): Solar activity dependence of total
473 electron content derived from GPS observations over Mbarara. *Advances in Space
474 Research*. **50**, 415– 426.

475 Akala, A.O., E O Oyeyemi, E O Somoye, A B Adeloye, and A.O., Adewale. 2010. Variability of
476 foF2 in the African Equatorial Ionosphere. *Advances in Space Research* 45 (11). COSPAR:
477 1311–14. doi:10.1016/j.asr.2010.01.003.

478 Andreeva, E. S., and M. V Lokota. 2013. Analysis of the Parameters of the Upper Atmosphere
479 and Ionosphere Based on Radio Occultation, Ionosonde Measurements, IRI and NeQuick
480 Model Data. 52(10):1820–26. doi.org/10.1016/j.asr.2013.08.012.

481 Aravindan, P., and Iyer, K. N. (1990): Day-to-day variability in ionospheric electron content at
482 low latitudes, *Pmet. Space Sci.*, **38**(6),743-750.

483 Bagiya, Mala S, H.P Joshi, K N Iyer, M Aggarwal, S Ravindran, and B M Pathan. 2009. "TEC
484 Variations during Low Solar Activity Period (2005-2007) near the Equatorial Ionospheric
485 Anomaly Crest Region in India." *Annales Geophysicae* 27: 1047–57. doi:10.5194/angeo-
486 27-1047-2009.

487 Balan, N., and Rao, P. B. (1984): Relationship Between Nighttime Total Electron Content
488 Enhancements, *Journal of Geophysical Research*, **89**(10), 9009-9013.

489 Balan, N., Iyer, K.N. Equatorial anomaly in ionospheric electron content and its relation to
490 dynamo currents. *J. Geophys. Res.* 88 (A12), 10259– 10262, 1983.

491 Bandyopadhyay, P. (1970): Measurement of total electron content at Huancayo, Peru, *Planet.
492 Space Sci.*, **18**, 129–135, doi:10.1016/0032-0633 (70)90150-9.

493 Belehaki, A Jankowski, N.Reinisch B. W. 2004. "Plasmaspheric Electron Content Derived from
494 GPS TEC and Digisonde Ionograms." 33:833–37.

495 Belehaki, A Jankowski, N.Reinisch B. W. 2004. "Plasmaspheric Electron Content Derived from
496 GPS TEC and Digisonde Ionograms." 33:833–37.

497 Belehaki, A., and Kersley, L. (2003): Statistical validation of the ITEC parameter, Third
498 Workshop of the COST271 Action, 23-27 September 2003, Spetses, Greece.

499 Bent, R.B., Llewellyn, S.K. and Schmid, P.E., 1972. A highly successful empirical model for the
500 worldwide ionospheric electron density profile. DBA Systems, Melbourne, Florida.

501 Bidaine, B. and R. Warnant. 2011. "Ionosphere Modelling for Galileo Single Frequency Users :
502 Illustration of the Combination of the NeQuick Model and GNSS Data Ingestion." *Advances in Space Research* 47(2):312–22. doi.org/10.1016/j.asr.2010.09.001).

503 Bilitza, D. (2001): 'International Reference Ionosphere 2000', *Radio Science*, **36**(2), 261-275.



505 Bilitza, D. (1986): International reference ionosphere: Recent developments, *Radio Science*, **21**,
506 343-346.

507 Bilitza, D., and Rawer, K. (1998): "International Reference Ionosphere Model (IRI- 93),"
508 <http://envnet.gsfc.nasa.gov/Models/EnviroNET-Models.html> *Adv. Space Res.*, **69**, 520-
509 829.

510 Bolaji, O. S., Adeniyi, J. O., Radicella, S. M., and Doherty, P. H. (2012): Variability of total
511 electron content over an equatorial West African station during low solar activity.
512 *RADIO SCIENCE*, **47**, RS1001 doi:10.1029/2011RS004812.

513 Breed, A.M, G L Goodwin, A-m Vandenberg, E A Essex, K J W Lynn, and Abstract
514 Ionospheric. 1997. Ionospheric Total Electron Content and Slab Thickness J . H . Silby 32
515 (4): 1635-43. 10.1029/97RS00454 2006.

516 Carlson, H.C. Incoherent scatter radar mapping of polar electrodynamics. *J. Atmos. Solar-Terr.
517 Phys.* 58 (1-4), 37-56, 1996.

518 Cherniak, Iurii and Irina Zakharenkova. 2016. NeQuick and IRI-Plas Model Performance on
519 Topside Electron Content Representation: Spaceborne GPS Measurements. 1-15.

520 Ciraolo, L., and P. Spalla. 1997. "Comparison of Ionospheric Total Electron Content from Navy
521 Navigation Satellite System and the GPS." *Radio Science* 32 (3): 1071-1080.
522 doi:10.1029/97RS00425.

523 Coïsson, P., Radicella, S.M., Leitinger, R. and Nava, B., 2006. Topside electron density in IRI
524 and NeQuick: features and limitations. *Advances in Space Research*, 37(5), pp.937-942.

525 Davies, K., Recent progress in satellite radio beacon studies with particular emphasis on the
526 ATS-6 Radio Beacon Experiment, *Space Sci. Rev.*, 25, 357-430, 1980

527 Ezquer, R. G., Adler, N.O., Radicella, S.M., Gonzalez, M .M., and Manza, J . R. (1992): Total
528 electron content obtained from ionogram data alone, *Radio Science*, **27**(3), 429-434.

529 Fox, M. W., and McNamara, L. F. (1988): Improved world-wide maps of monthly median
530 foF₂, *Journal of Atmospheric and Terrestrial Physics*, **50**, 1077-1086.

531 Huang, X., Reinisch, B.W. Vertical total electron content from ionograms in real time. *Radio
532 Sci.* 36 (2), 335-342, 2001. Ionization Anomaly over Africa Using Data Ingestion."
533 60:1732-38.

534 Jee, G., Schunk, R.W. and Scherliess, L., 2005. On the sensitivity of total electron content (TEC)
535 to upper atmospheric/ionospheric parameters. *Journal of atmospheric and solar-terrestrial
536 physics*, 67(11), pp.1040-1052.

537 Jesus, R De, P R Fagundes, A Coster, O S Bolaji, J H A Sobral, I S Batista, AJ De Abreu, et al.
538 2016. Effects of the Intense Geomagnetic Storm of September – October 2012 on the
539 Equatorial, Low- and Mid-Latitude F Region in the American and African Sector during the
540 Unusual 24th Solar Cycle." *Journal of Atmospheric and Solar-Terrestrial Physics* 138-139.
541 Elsevier: 93-105. doi:10.1016/j.jastp.2015.12.015.

542 Jodogne J.-C., H. Nebdi, and R.Warnan. 2004. Advances in Radio Science GPS TEC and ITEC
543 from Digisonde Data Compared with NEQUICK Model. 269-73.

544 Karia, S.P., and Pathak, K.N.(2011): GPS based Tec measurement for a period Aug 2008-Dec
545 2009 near the northern crest of India equatorial ionospheric anomaly region. *Journal of
546 earth system science*, **120**.5, 851-858.

547 Kenpankho, P., P. Supnithi, and T. Nagatsuma. 2013. ScienceDirect Comparison of Observed
548 TEC Values with IRI-2007 TEC and IRI-2007 TEC with Optional Fo F2 Measurements
549 Predictions at an Equatorial Region, Chumphon, Thailand. *Advances in Space Research*
550 Kenpankho, P., P. Supnithi, and T. Nagatsuma. 2013. ScienceDirect Comparison of Observed



551 TEC Values with IRI-2007 TEC and IRI-2007 TEC with Optional Fo F2 Measurements
552 Predictions at an Equatorial Region, Chumphon, Thailand. *Advances in Space Research*
553 Kumar, S., and Singh, A.K. (2009): Variation of ionospheric total electron content in Indian
554 low latitude region of the equatorial anomaly during May 2007–April 2008, *Advances*
555 in Space Research **43**, 1555–1562.

556 Langley, R., M. Fedrizzi, E. Paula, M. Santos, and A. Komjathy (2002), Mapping the low
557 latitude ionosphere with GPS, *GPS World*, 13(2), 41–46.

558 Leong, S. K. et al. 2014. Assessment of Ionosphere Models at Banting: Performance of IRI-
559 2007, IRI-2012, and NeQuick 2 Models during the Ascending Phase of Solar Cycle 24.
560 *Advances in Space Research* (2013) <http://dx.doi.org/10.1016/j.asr.2014.01.026>.

561 Liu, J. Y., H. F. Tsai, and T. K. Jung (1996b), Total electron content obtained by using the global
562 positioning system, *Terr. Atmos. Oceanic Sci.*, 7, 107.

563 Mala, S., Bagiya, H. P., Joshi, K. N., Iyer, M., Aggarwal, S., Ravindran, and Pathan, B.M.
564 (2009): TEC variations during low solar activity period (2005–2007) near the equatorial
565 Ionospheric Anomaly Crest region in India, *Ann. Geophys.*, **27**, 1047–1057.

566 Mannucci, A. J., B. D. Wilson, and C. D. Edwards (1993), A new methodfor monitoring the
567 Earth' s ionospheric total electron content using the GPS global network, paper
568 presented at ION GPS - 93, Inst. of Navigation., pp. 1323–1332, Salt Lake City, Utah,
569 22–24 Sept.

570 Mckinnell, Lee-anne, Ben Opperman, and Pierre J. Cilliers. GPS TEC and Ionosonde TEC over
571 Grahamstown, South Africa: First Comparisons Lee-Anne McKinnell, Ben Opperman and
572 Pierre J. Cilliers. (April 1996).

573 McNamara, L.F (1985). The use of total electron content measurements to validate empirical
574 models of the ionosphere. *Adv. Space Res.* **5** (7), 81– 90.

575 Migoya Orué, Y. O., S. M. Radicella, P. Coisson, R. G. Ezquer, and B. Nava. 2008. Comparing
576 TOPEX TEC Measurements with IRI Predictions.” *Advances in Space Research* 42(4):757–
577 62.

578 Migoya-Orue, Y., O. Folarin-olufunmilayo, S. Radicella, K. Alazo-Cuertas, and A. B. Rabiu.
579 2017. “ScienceDirect Evaluation of NeQuick as a Model to Characterize the Equatorial
580 Mosert, M, L A McKinnell, M Gender, C Brunini, J Araujo, R G Ezquer, and M Cabrera. 2007.
581 “Variations of F O F 2 and GPS Total Electron Content over the Antarctic Sector,” 327–33.
582 doi:10.5047/eps.2011.01.006.

583 Mosert, M. and D. Altadill. 2007. “Comparisons of IRI TEC Predictions with GPS and
584 Digisonde Measurements at the Ebro.” 39:841–47.

585 Nava, B. and S. M. Radicella. 2009. “On the Use of NeQuick Topside Option in IRI-2007.”
586 43:1688–93.

587 Obrou, O.K., Mene, M.N., Kobea, A.T., and Zaka, K.Z. (2008): Equatorial total electron content
588 (TEC) at low and high solar activity, *Advances in Space Research* **43**, 1757–1761.

589 Okoh, D., McKinnell, L.A., Cilliers, P., Okere, B., Okonkwo, C. and Rabiu, B., 2015. IRI-vTEC
590 versus GPS-vTEC for Nigerian SCINDA GPS stations. *Advances in Space Research*, 55(8),
591 pp.1941-1947.

592 Olatunji, E. O. (1967): The total columnar electron content of the equatorial ionosphere,
593 Olwendo, O. J., P. Baki, P. J. Cilliers, C. Mito, and P. Doherty. 2013. “Comparison of GPS TEC
594 Variations with IRI-2007 TEC Prediction at Equatorial Latitudes during a Low Solar
595 Activity (2009-2011) Phase over the Kenyan Region.” *Advances in Space Research* 52(10).

596 Olwendo, O. J., P. Baki, P. J. Cilliers, C. Mito, and P. Doherty. 2012. “Comparison of GPS TEC



597 Measurements with IRI-2007 TEC Prediction over the Kenyan Region during the
598 Descending Phase of Solar Cycle 23." Advances in Space Research 49(5):914–21.
599 Retrieved (<http://dx.doi.org/10.1016/j.asr.2011.12.007>).

600 Olwendo, O. J., P. Baki, P. J. Cilliers, C. Mito, and P. Doherty. 2013. "Comparison of GPS TEC
601 Variations with IRI-2007 TEC Prediction at Equatorial Latitudes during a Low Solar
602 Activity (2009-2011) Phase over the Kenyan Region." Advances in Space Research 52(10).

603 Olwendo, O.J., Baki, P., Cilliers, P.J., Mito, C., and Doherty, P. (2012): Comparison of GPS
604 TEC measurements with IRI-2007 TEC prediction over the Kenyan region during the
605 descending phase of solar cycle 23, Advances in Space Research **49**, 914–921.

606 Rabiu, A. B., A. O. Adewale, R. B. Abdulrahim, and E. O. Oyeyemi. 2014. "ScienceDirect TEC
607 Derived from Some GPS Stations in Nigeria and Comparison with the IRI and NeQuick
608 Models." Advances in Space Research 53(9):1290–1303. Retrieved
609 (<http://dx.doi.org/10.1016/j.asr.2014.02.009>).

610 Radicella, S.M., Bilitza, D., Reinisch, B.W., and Adeniyi, J.O., Mosert Gonzalez, M.E., Zolesi,
611 B., Zhang, M.L., Zhang, S. (1998): IRI Task Force Activity At ICTP: Proposed
612 Improvements For The IRI Region Below The F Peak, Adv. Space Res. **22**(6) 731-739.

613 Rama Rao, P.V.S., Gopi Krishna, S., Niranjan, K., Prasad, D.S.V.V.D. Temporal and spatial
614 variations in TEC using simultaneous measurements from the Indian GPS network of
615 receivers during the low solar activity period of 2004–2005. Ann. Geophys. **24**, 3279–
616 3292, 2006b.

617 Rama Rao, P.V.S., Niranjan, K., Prasad, D.S.V.V.D., Gopi Krishna, S., Uma, G. On the validity
618 of the ionospheric pierce point (IPP) altitude of 350 km in the equatorial and low latitude
619 sector. Ann. Geophys. **24**, 2159–2168, 2006a.

620 Rastogi, R G., and Sharma, R. P. (1971): Ionospheric electron content at Ahmedabad (near the
621 crest of the equatorial anomaly) by using beacon satellite transmissions during half a
622 solar cycle; Planet. Space Sci. **19** 1505–1517.

623 Rastogi, R.G., Iyer, K.N. and Bhattacharyya, J.C., 1975. Total electron content of the ionosphere
624 over the magnetic equator. Current Science, pp.531-533.

625 Rawer, K. and Bilitza, D., 1990. International Reference Ionosphere—plasma densities: status
626 1988. Advances in space research, 10(8), pp.5-14

627 Rawer, K., Lincoln, J. V., and Conkright, R. O. (1981): International Reference Ionosphere—
628 IRI 79, World Data Center A for Solar-Terrestrial Physics, Report UAG-82, Boulder,
629 Colorado. **52**. 223-232.

630 Reinisch, B.W., Huang, X. Deducing topside profile and total electron content from bottomside
631 ionograms. Adv. Space Res. **27** (1), 23–30, 2001.

632 Rios, V.H., Medina, C.F. and Alvarez, P., 2007. Comparison between IRI predictions and
633 digisonde measurements at Tucuman. Journal of Atmospheric and Solar-Terrestrial Physics,
634 **69**(4-5), pp.569-577.

635 Rush, C., Fox, M., Bilitza, D., Davies, K., McNamara, L., Stewart, F., and PoKempner, M.
636 (1989): Ionospheric mapping: an update of foF2 coefficients, Telecomm. J. **56**, 179 182.

637 Skinner, N. J. (1966): Measurements Of Total Electron Content Near The Magnetic Equator,
638 Planet. Space Sci. Vol. **14**, Pp. 1123 - 1129.

639 Tan, A, and Newberry College. 1982. "On the Nighttime Increase of" 44.

640 Tariku, Yekoye. 2015. "Patterns of GPS-TEC Variation over Low-Latitude Regions (African
641 Sector) during the Deep Solar Minimum (2008 to 2009) and Solar Maximum (2012 to
642 2013) Phases." Earth, Planets, and Space **67** (1). doi:10.1186/s40623-015-0206-2.



643 Tyagi, T. R., Yeh, K. C., and Tauriainen, A. (1982): The Electron Content and Its Variations at
644 Natal, Brazil, *Journal of Geophysical Research*, **87**(A4), 2525-2532.

645 Wu C-C, Liou K., Shan, S. J., and Tseng, C. L. (2008): Variation of ionospheric total electron
646 content in Taiwan region of the equatorial anomaly from 1994 to 2003, *Advances in
647 Space Research* **41**, 611–616.

648 Young, D. M. L., Yuf, P. C., and Roelofs, T.H.(1970): Anomalous nighttime increases in total
649 electron content, *Planet. Space Sci.* **18**, 1163-1179.

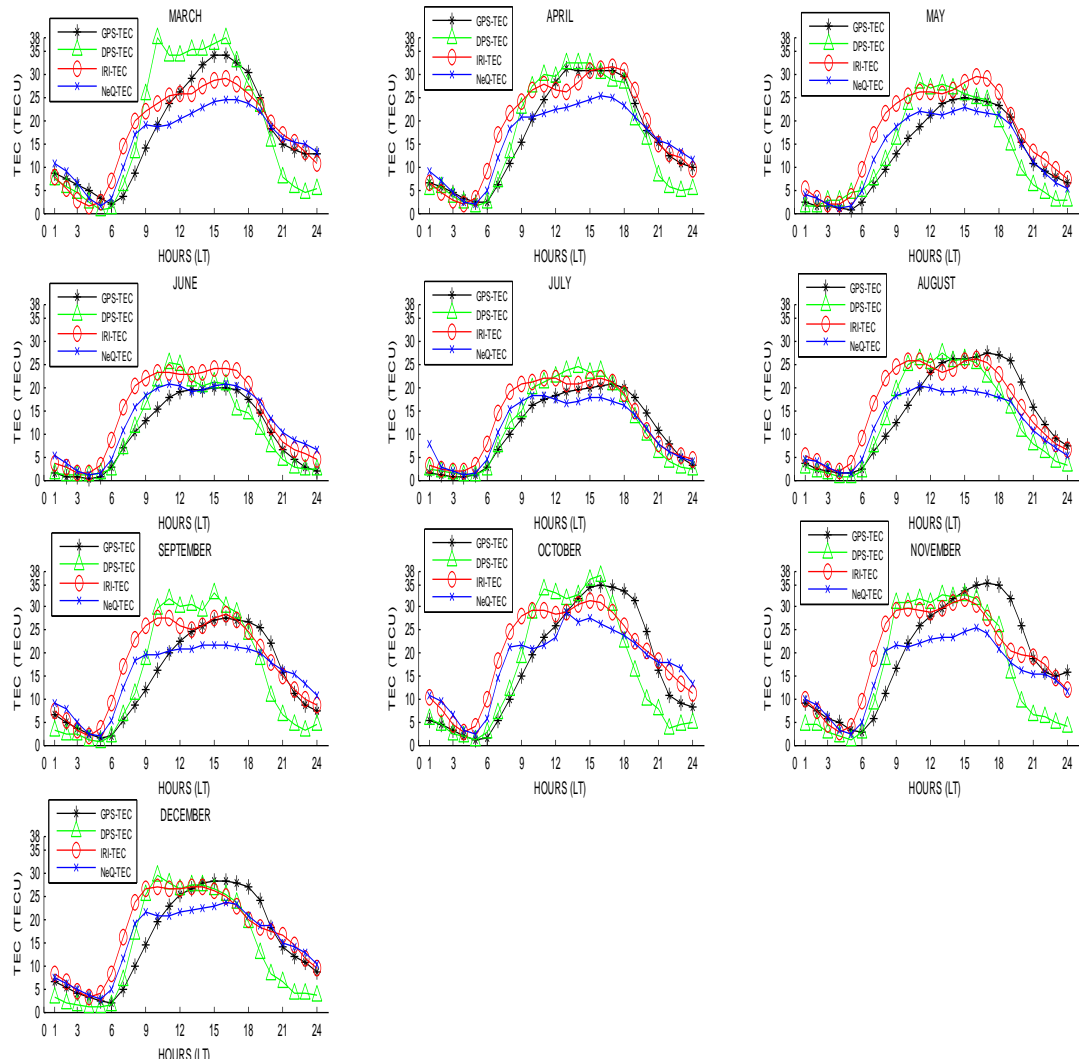
650 Yu, Xiao, Chengli Shi, Dun Liu, and Weimin Zhen. 2012. "A Preliminary Study of the NeQuick
651 Model over China Using GPS TEC and Ionosonde Data." 2012 10th International
652 Symposium on Antennas, Propagation and EM Theory, ISAPE 2012 (36):627–30.

653 Zh, A. G.Noordwijk, Campus Nord, Mod C-, and Jordi Girona 2014. "NeQuick Model,
654 GALILEO, Slant TEC, Modified Dip, Effective Ionisation Level." (2).

655 Zhang, Man Lian, Sandro M. Radicella, Jian Kui Shi, Xiao Wang, and Shun Zhi Wu. 2006.
656 "Comparison among IRI, GPS-IGS and Ionogram-Derived Total Electron Contents."
657 *Advances in Space Research* 37(5):972–77.

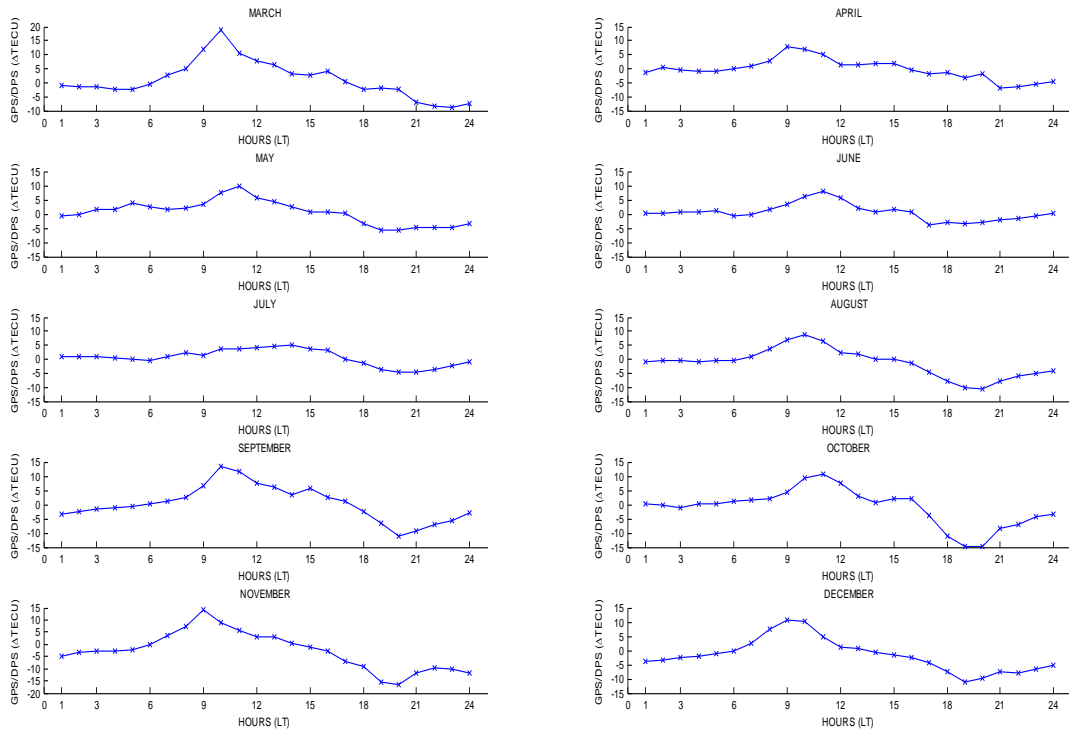
658

659
660 **7.0 Figures**
661



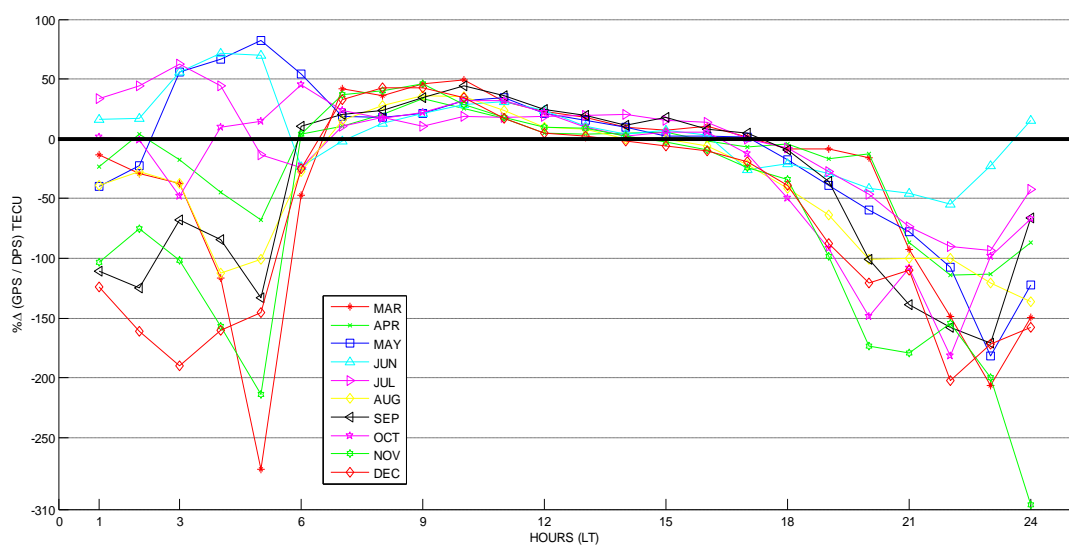
662
 663
 664

Figure 1. The hourly variations of the monthly median of GPS, DPS, IRI, and NeQuick TEC in March-December during quiet period.



665
 666
 667
 668

Figure 2a. The hourly Δ TEC variations between the GPS-TEC and DPS-TEC from March - December during quiet period.

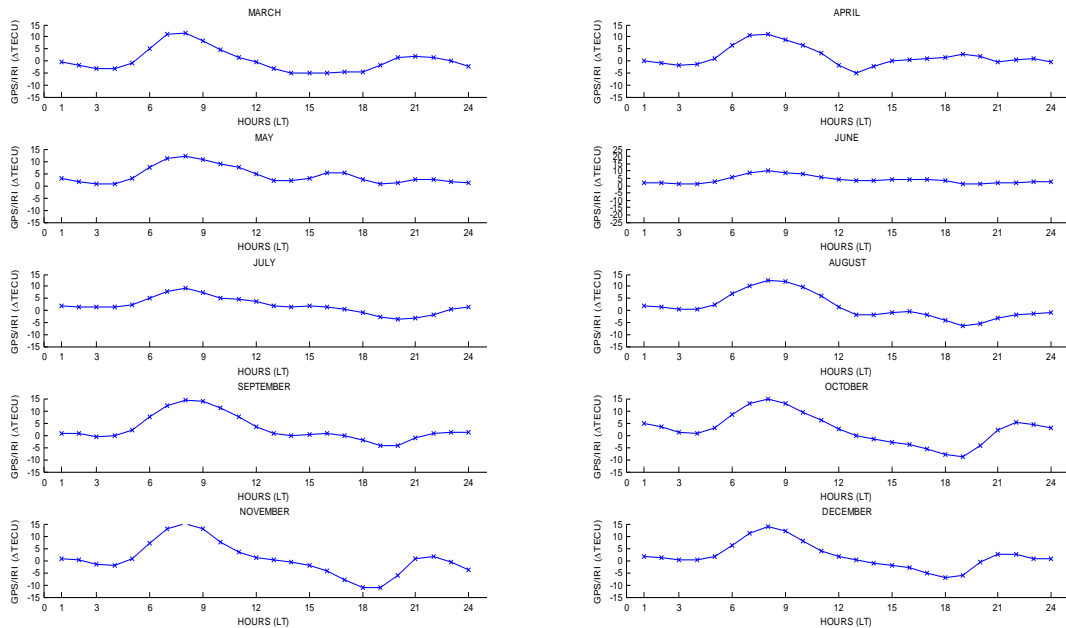


669
 670
 671
 672

Figure 2b. The mass plot of the hourly Δ TEC variations between the GPS-TEC and DPS-TEC from March - December during quiet period.

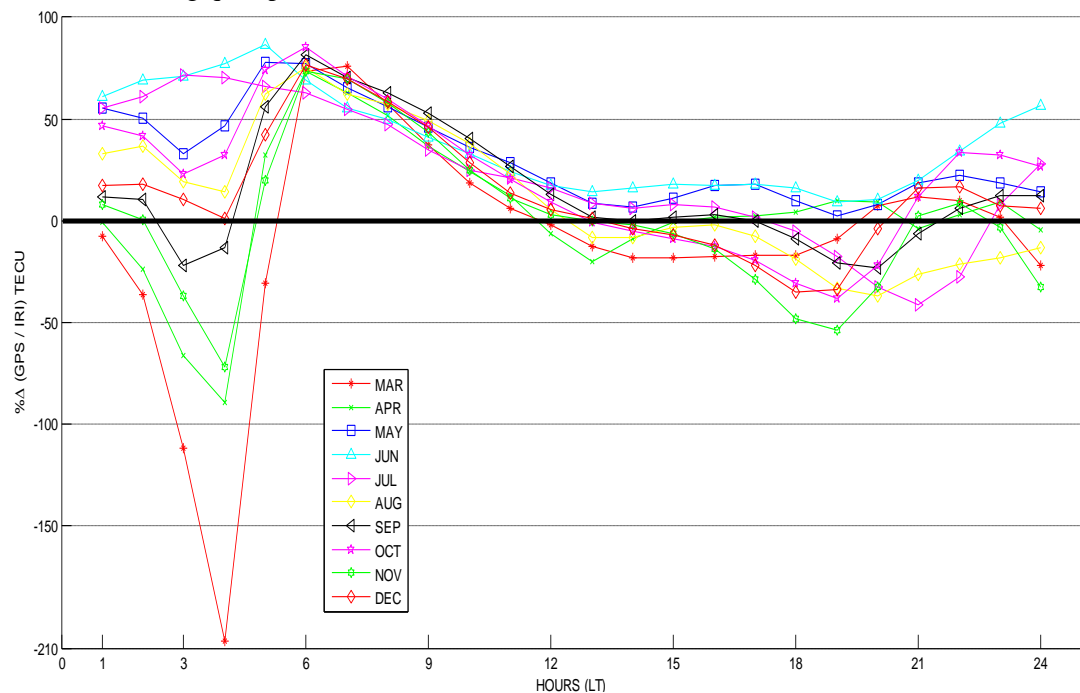


673



674
 675
 676

Figure 3a. The hourly Δ TEC variations between the GPS-TEC and IRI-TEC from March - December quiet period.

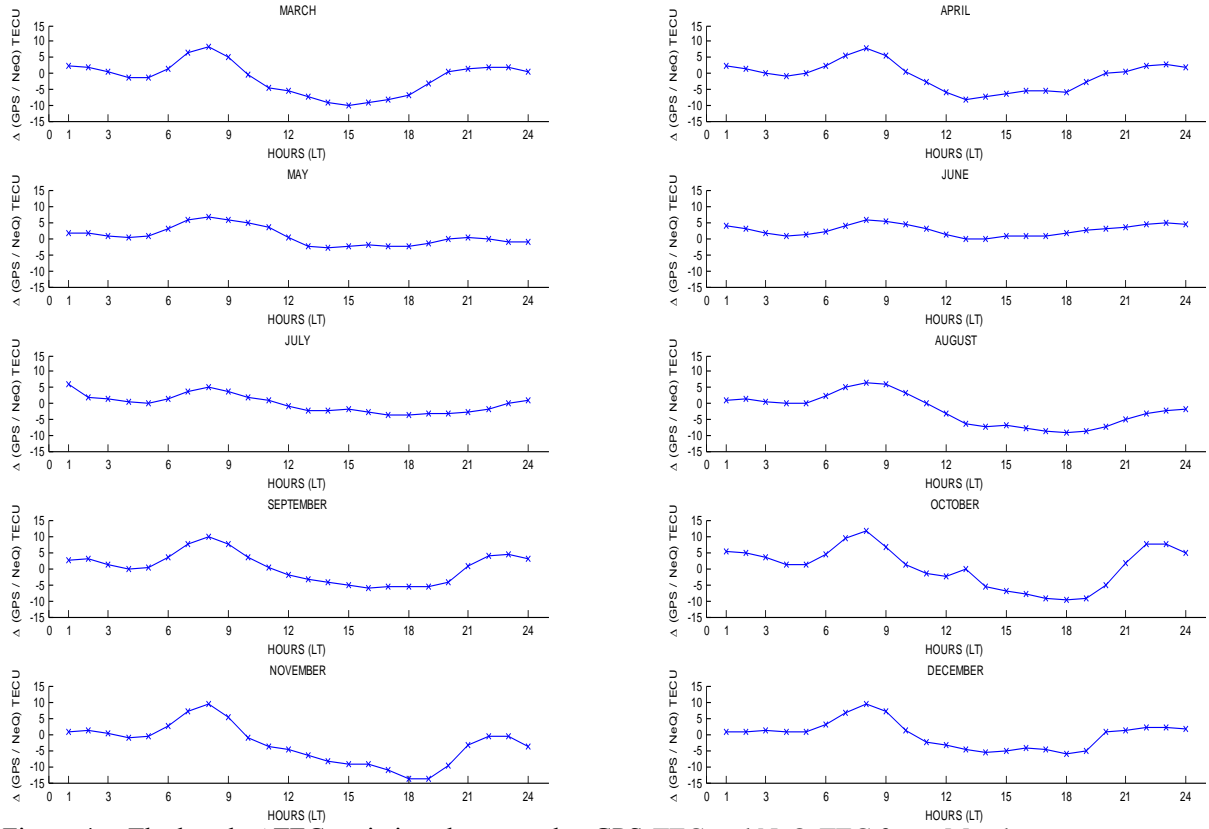


677
 678
 679

Figure 3b. The mass plot of the hourly Δ TEC variations between the GPS-TEC and IRI-TEC from March to December quiet period.

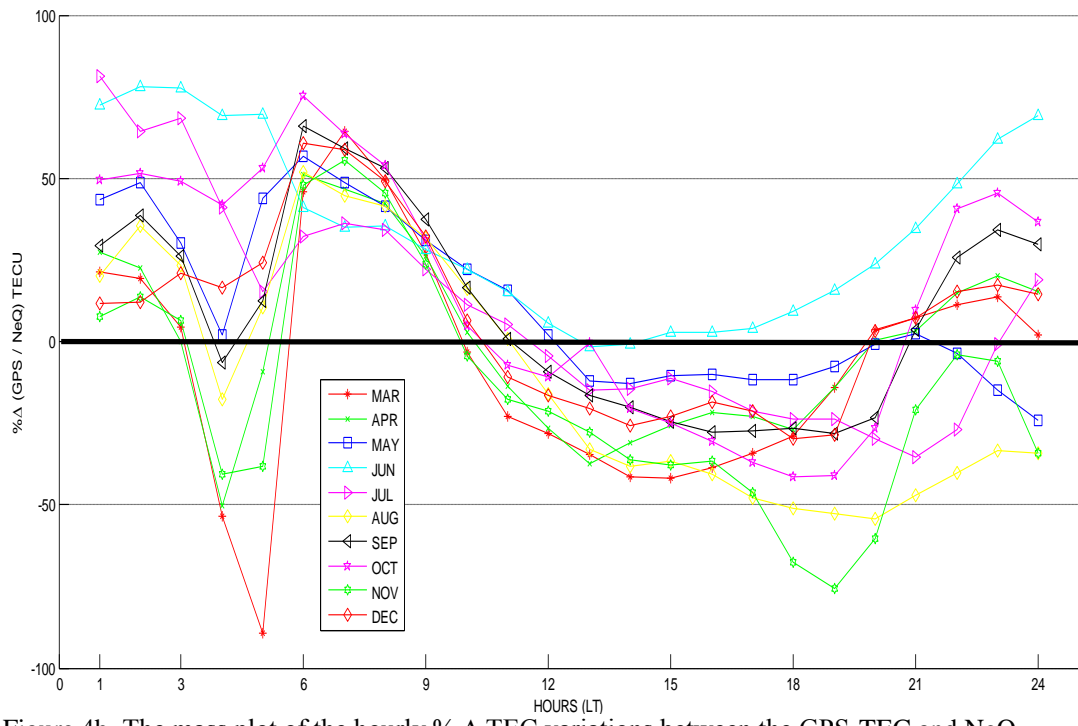


680
681
682
683

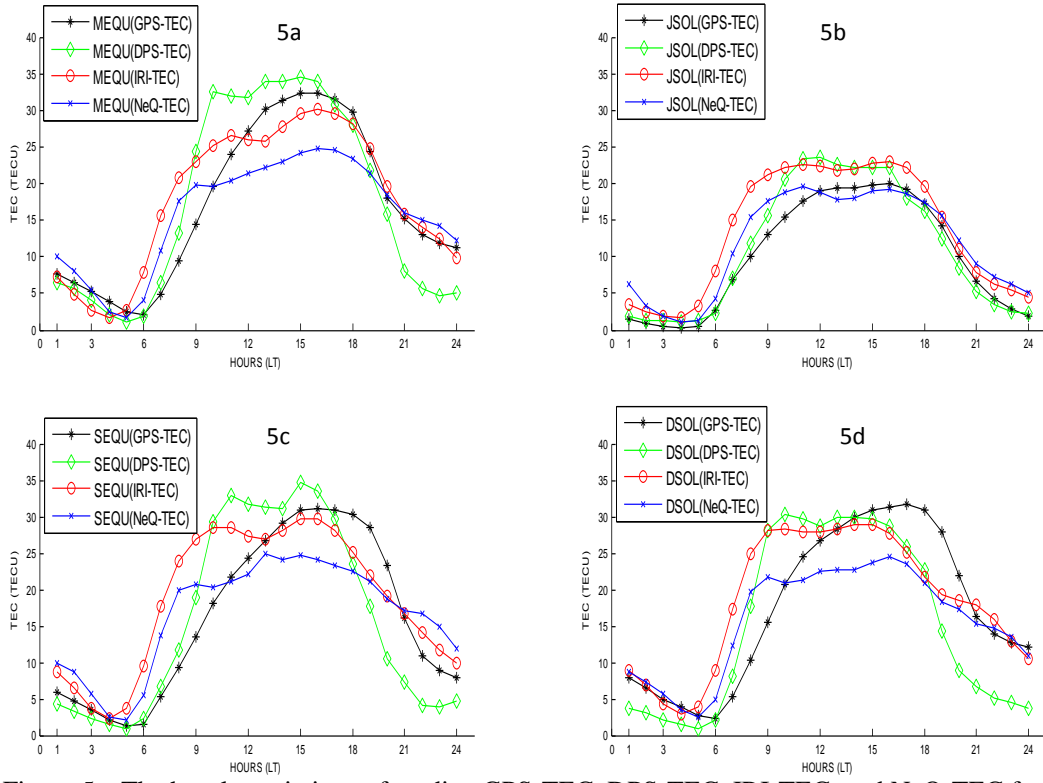


684
685
686
687
688

Figure 4a. The hourly Δ TEC variations between the GPS-TEC and NeQ-TEC from March - December during quiet period.



689
690 Figure 4b. The mass plot of the hourly $\% \Delta$ TEC variations between the GPS-TEC and NeQ-
691 TEC from March - December during quiet period
692
693
694
695



696
 697 Figure 5a. The hourly variations of median GPS-TEC, DPS-TEC, IRI-TEC,
 698 and NeQ-TEC for
 699 March equinox during quiet period.
 700 Figure 5b. The hourly variations of median GPS-TEC, DPS-TEC, IRI-TEC,
 701 and NeQ-TEC for
 702 June solstice during quiet period.
 703 Figure 5c. The hourly variations of median GPS-TEC, DPS-TEC, IRI-TEC,
 704 and NeQ-TEC for
 705 December solstice during quiet period.